JOURNAL OF GEOPHYSICAL RESEARCH, VOL. 87, NO. C1, PAGES 469–481, JANUARY 20, 1982

Movable Bed Roughness in Unsteady Oscillatory Flow

WILLIAM D. GRANT

Ocean Engineering Department, Woods Hole Oceanographic Institution
Woods Hole, Massachusetts 02543

OLE SECHER MADSEN

Civil Engineering Department, Massachusetts Institute of Technology
Cambridge, Massachusetts 02139

A model to predict the roughness in unsteady oscillatory flows over movable, noncohesive beds is presented. The roughness over movable beds is shown to be a function of the boundary shear stress, rather than a fixed geometrical scale as is the case for fully rough turbulent boundary shear flows over immobile beds. The model partitions the roughness into two distinct contributions. These two contributions are due to the form drag around individual bed forms and to the near-bed sediment transport. The form drag over the bed forms is treated explicitly as a function of the boundary geometry and shear stress. The ripples are predicted as a function of the local skin friction, and a semiempirical expression is derived using standard law-of-the-wall arguments, which gives the ripple or form roughness as a function of the boundary geometry. The ripple roughness is found to be proportional to the product of the ripple steepness and height. Favorable comparison of the form drag model with the results of Bagnold's (1946) fixed ripple study is found. The value of z_0 associated with intense sediment transport in oscillatory flow over a flat bed is determined from Carstens et al.'s (1969) experiments. This value is found to be 7 or 8 grain diameters. An expression is derived for the roughness associated with the maximum thickness of a near-bottom sediment-transporting layer consistent with Owen's (1964) roughness hypothesis for saltation of uniform grains in air. At large values of the boundary shear stress relative to the critical value for initial sediment motion, the derived expression is similar to the results of Smith and McLean's (1977) unidirectional flow approach modified for oscillatory flow. The total roughness model is found to compare favorably with Carstens et al.'s (1969) data. In contrast to Smith and McLean's (1977) steady flow findings, the results here show that when ripples are present, they account for a significant portion of the boundary roughness.

INTRODUCTION

The friction developed at the seabed plays an important role in many physical processes occurring on the continental shelf. These processes include shelf currents, bottom boundary layer flows, the generation and propagation of shallow water surface gravity waves, and sediment transport phenomena. Moreover, the behavior of benthic biota and chemistry of the seawater-sediment interface are strongly related to the mixing which occurs in the immediate vicinity of the bottom. This mixing depends on fluid shear caused by friction at the seabed. Accurate models of the boundary shear stress are required for successful modeling of frictionally dominated processes. It is well known that the boundary shear stress depends upon the roughness of the boundary. Specification of the roughness for unidirectional flow over fixed rough surfaces has been extensively studied (see *Wooding et al.* [1973] for a review of the drag of rough surfaces on fully developed turbulent shear flow), and a wide range of experimental data exist which quantify the effect of various roughness arrays on the wall shear flow. The concept of an 'equivalent sand grain roughness height,' k_s, evolved from the pioneering work of *Nikuradse* [1933]. Using this concept, the roughness height, determined experimentally, is expressed in terms of a fixed dimension of the roughness elements. The roughness height is a constant for similar geometry, and for fully rough turbulent flow, when k_s is correctly nondimensionalized by the characteristic length scale for the flow, it uniquely determines the friction coefficient expressing the ratio of shear velocity to fluid velocity.

Paper number 1C1441.
0148-0227/82/001C-1441$01.00

Recent field measurements, such as those of *Smith and McLean* [1977] and *Dyer* [1980], made in turbulent shear flows over bottoms of sand, silt, or mud, indicate that fixed bed roughness models do not always explain the observed roughness magnitudes. The discrepancy between fixed bed models and field observations can be explained by movable bed effects. It is well established that where sediment transport occurs, bed forms develop and are modified in response to the boundary shear flow. *Owen* [1964] hypothesized for aeolian flows above a layer of saltating sediment that the flow sees the layer as a solid wall roughness and that this roughness is comparable to the depth of the saltation layer. *Smith and McLean* [1977] adopted *Owen*'s [1964] hypothesis to explain the hydrodynamic roughness over a sand bottom in the Columbia River. They developed an expression for the roughness consisting of two contributions: the Nikuradse sand grain roughness and the roughness associated with the thickness of the bed load layer. The roughness is a function of the boundary shear stress, rather than a constant quantity set by a fixed roughness geometry, according to *Smith and McLean*'s [1977] result.

Oscillatory currents caused by surface wind waves, in addition to other relatively steady currents, influence much of the bottom on the continental shelf. No equivalent model to *Smith and McLean*'s [1977] unidirectional flow roughness model exists for such unsteady oscillatory flows. The purpose of this paper is to present a model which accounts for movable bed effects on the friction over sand bottoms subjected to the action of surface gravity waves. Quantitative comparisons of the model with pure oscillatory flow are possible using the existing data base. For typical combined

wave and current flows on the shelf most of the sediment resuspension will be due to the waves [cf. *Grant and Madsen,* 1979*a*]. As long as the maximum near-bed orbital wave velocity is greater than the magnitude of the mean current in the immediate vicinity of the wave boundary layer, the bed forms may be expected to be wave-dominated, i.e., symmetrical wave-formed ripples. Thus it is argued that the model presented here can be extended to provide qualitative insight into the combined flow case.

Here the boundary roughness is assumed to be made up of two primary contributions, similar to the *Smith and McLean* [1977] model which inspired this work. These two contributions are due to the form drag around individual bed forms and to the near-bed sediment transport. The model is more detailed than *Smith and McLean*'s [1977] model, however. The form drag over the bed forms is treated explicitly as a function of the boundary geometry and skin friction. By using standard law-of-the-wall arguments a semiempirical expression is derived giving the ripple or form roughness as a function of the boundary geometry. An expression relating z_0 to the maximum thickness of a near-bed sediment transporting layer is developed based on *Owen*'s [1964] roughness hypothesis for saltation of uniform grains. The expression explicitly includes the relative density of the sediment and the effect of added mass on the proportionality constant between z_0 and the layer thickness.

The prediction of boundary shear stress in unsteady oscillatory flow is a complex problem. The approach adopted here borrows from semiempirical models of turbulence used in steady, unidirectional flows with appropriate modifications due to the unsteadiness of the flow and the presence of pressure gradients. References to steady flow analogies are provided where possible.

BACKGROUND

A theory relating boundary roughness to the boundary shear stress is needed to determine the bottom friction due to an oscillatory flow over a movable bed. The boundary roughness then must be related to the physical characteristics of the boundary, i.e., grain size, bed form geometry, and sediment transport. Knowledge of the behavior of the seabed under waves is necessary to accomplish this second task. Seabed conditions can be related to the boundary roughness using similarity arguments, conservation laws, and an empirically determined proportionality constant. To facilitate the subsequent model development and discussion, a brief description is given here of (1) a friction model for oscillatory flow, (2) the response of a sand bed to an oscillatory boundary shear flow, and (3) two data sets used in the model development.

Friction under waves. The boundary shear stress under a wave, τ_b, can be defined on the basis of *Jonsson*'s [1966] work as

$$\tau_b = \tfrac{1}{2}\rho f_w u_{bm}^2 \,|\sin(\omega t + \phi)|\sin(\omega t + \phi) \tag{1}$$

where f_w is the wave friction factor; ρ is the fluid density; u_{bm} is the near-bottom orbital wave velocity amplitude; ω is the radian wave frequency, equal to $2\pi/T$ (where T is the wave period); t is time; and ϕ is the phase shift between u_{bm} and the maximum shear stress. For fully rough turbulent flows (the only case considered here) the friction factor in (1) is a function of only the relative boundary roughness k_b/A_b where A_b is the near-bottom excursion amplitude of a fluid particle undergoing simple harmonic motion of radian frequency ω. From linear wave theory,

$$A_b = H/2 \sinh kh \tag{2}$$

in which H is the wave height; h is the water depth; k is the wave number, equal to $2\pi/L$ where L is the wave length; and k_b is an 'equivalent roughness height.' Thus f_w relates the boundary shear stress to the roughness of the boundary.

Grant and Madsen [1979*a*] have derived an expression relating the friction factor and the relative roughness for combined waves and currents in fully rough turbulent flow. A relationship between f_w and k_b/A_b can be found by taking the theory in the limiting case of a pure wave motion as

$$f_w = 0.08/[\mathrm{Ker}^2\, 2(\zeta_0)^{1/2} + \mathrm{Kei}^2\, 2(\zeta_0)^{1/2}] \tag{3}$$

which is valid for $k_b/A_b \leq 1$. The subscript w denotes that only a wave motion is being considered; ζ_0 is a dimensionless roughness length

$$\zeta_0 = k_b/30l \tag{4}$$

and l is the characteristic scale of the wave boundary layer given by

$$l = \kappa u_{*wm}/\omega \tag{5}$$

in which k is von Karman's constant and u_{*wm} is the magnitude of the maximum shear velocity under the wave expressed by

$$u_{*wm} = (f_w/2)^{1/2} u_{bm} \tag{6}$$

and Ker and Kei are Kelvin functions of zero order.

The preceding relationship implicitly assumes the length scale of the turbulent eddies to be the boundary roughness k_b. For values of $k_b/A_b > 1$, the eddy length scale will be the particle excursion amplitude A_b rather than the bottom roughness k_b. This leads to the argument that f_w is a constant for $k_b/A_b > 1$, and this constant value is obtained by evaluating (3) for $k_b/A_b = 1$, i.e.,

$$f_w = 0.23 \qquad k_b/A_b > 1 \tag{7}$$

Relationships between the friction factor and boundary roughness for oscillatory flows have been developed by *Jonsson* [1966], *Kajiura* [1964], and *Kamphuis* [1975] using semiempirical, theoretical, and empirical approaches, respectively. *Grant and Madsen* [1979*b*] and *Grant* [1980] have compared (3) and (7) with the three pure wave models and found close agreement among the various approaches. The relationships given by (3) and (7) are valid for a fixed or movable bed provided that a suitable definition of the equivalent roughness length k_b is known. The use here of k_b is in analogy to the *Nikuradse* [1933] 'equivalent sand grain roughness.' The equivalent sand grain roughness is the sand diameter of a flat bed of uniform sand packed at maximum density that would result in the same flow resistance as that observed for a given roughness configuration. Whereas k_s is a constant for a given roughness geometry, k_b may vary as a function of the skin friction in the flow. The use of the equivalent roughness height makes it easy to compare the importance of movable bed effects on the flow resistance for a given boundary geometry with the same fixed bed geometry. Moreover, since only rough turbulent flow is considered here, the use of $k_b/30$ for the hydrodynamic roughness length z_0 makes comparison with fixed beds straightforward.

Movable beds under waves. Ripples start to form as the friction on the seabed increases from conditions just sufficient to initiate sediment motion. The instability mechanism that controls the bed forms is poorly understood; however, it is known that two distinct ranges of ripple growth and decay exist. In the first range, known as the equilibrium range, the ripple steepness (height to length ratio η/λ) is equal to or nearly equal to a maximum, and the ripple length scales with the near-bottom excursion amplitude of a fluid particle under the wave given by (2). A decrease in ripple steepness occurs with an increase in friction beyond the value at equilibrium. This decrease in steepness is associated with a lower ripple height, while a simultaneous decorrelation between excursion amplitude and ripple length occurs. This region, where (2) and the ripple length are no longer in equilibrium, is called the breakoff region. *Inman* [1957] first noted the existence of a transition between these two regions independent of any consideration of boundary shear stress. The point where this transition occurs will be referred to as the breakoff point. The ripples will be obliterated by the flow for sufficiently large values of the boundary shear stress. Moreover, in the breakoff range and beyond, the near-bed sediment transport rate is high, whereas equilibrium ripples occur at relatively low values of sediment transport.

Description of the geometry of the bed forms is not adequate by itself to determine the boundary roughness. The boundary shear stress must be related to the conditions at the bed; however, these change as a function of the shear stress. W. D. Grant et al. (manuscript in preparation, 1981) present an empirical analysis of the geometry of wave-formed ripples as a function of boundary shear stress, i.e., skin friction. By using their results the breakoff point can be predicted from the empirically derived expression

$$(\psi'/\psi_c)_B = 1.8 S_*^{0.6} \tag{8}$$

where ψ'/ψ_c is the ratio of the maximum value of Shields' parameter ψ' to the critical value for initiation of motion ψ_c [cf. *Madsen and Grant*, 1976, 1977].

$$\psi' = \tau_{bm}'/\rho(s-1)gd \tag{9}$$

where s is the relative density of the sediment, equal to ρ_s/ρ in which ρ_s is the sediment density; g is the acceleration of gravity; d is the sediment diameter; and τ_{bm}' is the maximum value of the skin friction under the wave,

$$\tau_{bm}' = \tfrac{1}{2}\rho f_w' u_{bm}^2 \tag{10}$$

with f_w' evaluated using the sand grain roughness. The use of primes in (9) denotes that Shields' parameter is based on the skin friction. S_* is a dimensionless sediment parameter [*Madsen and Grant*, 1976] given by

$$S_* = (d/4\nu)[(s-1)gd]^{1/2} \tag{11}$$

where ν is the kinematic viscosity of water. In (8) the subscript B denotes the breakoff point.

The parameter ψ'/ψ_c is useful in characterizing the behavior of the ripples and the subsequent sediment transport. In the equilibrium range the ripple steepness is nearly independent of the ratio ψ'/ψ_c; as the ripples decay, however, the steepness becomes dependent on the value of ψ'/ψ_c. The rate of sediment transport also increases with increasing ψ'/ψ_c. Figure 1 shows the ripple steepness plotted versus ψ'/ψ_c for *Carstens et al.*'s [1969] data (discussed below). The contrast in the behavior of the ripple steepness in the equilibrium

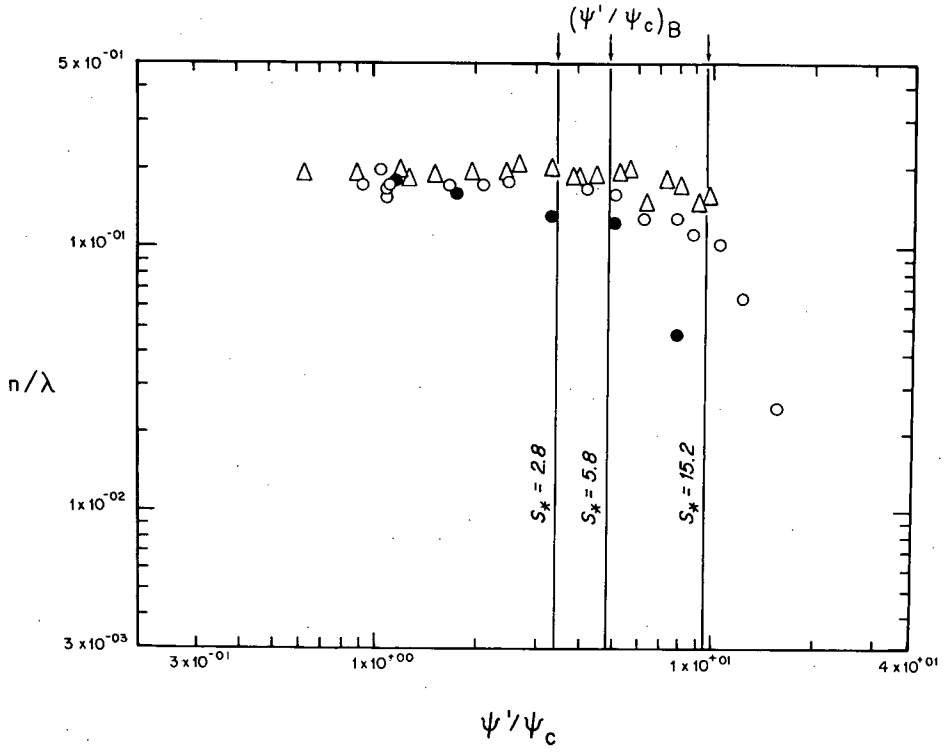

Fig. 1. Ripple steepness n/λ as a function of ψ'/ψ_c and S_* from *Carstens et al.*'s [1969] experiments. Note the distinct breakoff point for each value of S_*. The values of the breakoff point predicted from (8) are indicated. See Figure 3 for symbols.

region and the breakoff region is distinctly illustrated in the figure.

Using *Carstens et al.*'s [1969] data as well as several other data sources, W. D. Grant et al. (manuscript in preparation, 1981) fit straight lines to the values of the nondimensional ripple height η/A_b and ripple steepness plotted in the manner illustrated by Figure 1 to arrive at the empirical relationships for ripple geometry presented in Table 1.

Data for friction under waves. Various features of wave-formed ripples in beds of uniform sand were observed in a comprehensive laboratory study by *Carstens et al.* [1969], hereafter Carstens. Experiments were performed where the period of oscillation in a water tunnel was kept constant but the boundary shear stress was varied by changing the amplitude of the oscillatory water motion. The bed conditions in Carstens' experiments include the growth of ripples from an initially flat bed to a maximum steepness and then the subsequent decay of the ripples back to a flat bed with a large sediment transport over it. The additional energy dissipation for oscillatory flow over a rippled bed relative to a smooth flat bed was determined from measurements of work input into the water tunnel. Friction factors calculated from Carstens' data can be determined only in relation to the smooth flat bed friction factor. Friction factors for the rippled bed or high bed load transport runs are generally 2 orders of magnitude larger than the smooth fixed bed values; thus the relative values present no problems here. Carstens' experiments allow the total model for the movable bed roughness, i.e., ripple form drag plus near-bed sediment transport, to be established.

Bagnold [1946], hereafter Bagnold, determined the work done per oscillation in moving a rippled plate through the water. Two sets of artificial ripples were used in the study with respective crest-to-crest spacing of 10 and 20 cm and a steepness of approximately 0.15. The ripples were configured as two circular arcs intersecting to form a ripple crest with an angle of 120°. Runs were made over a range of plate oscillation amplitudes for each ripple type. The average drag on the plate can be calculated from the work, allowing a test of the form roughness model, developed here, independent of sediment transport effects.

For the two data sets described above, the value of the boundary shear stress is calculated from the average rate of energy dissipation $\overline{E}_{\text{dis}}$, given by [*Kajiura*, 1964]

$$\overline{E}_{\text{dis}} = \overline{\tau_b u_b} \tag{12}$$

where the overbar indicates time average over a wave cyle; u_b is the near-bottom orbital velocity under the wave given by linear wave theory as

$$u_b = u_{bm} \sin \omega t \tag{13}$$

and τ_b is the bottom shear stress under the wave, given by (1). *Putman and Johnson* [1949] ignore the possible phase shift between τ_{bm} and u_{bm} and obtain from (12)

$$\overline{E}_{\text{dis}} = (2/3\pi)\rho f_e u_{bm}^3 \tag{14}$$

where f_e is introduced as an energy dissipation factor. Substituting (13) and (1) into (12) and equating the result to (14) yields

$$f_w = f_e/\cos \phi \tag{15}$$

For rough turbulent flow over a flat bed the phase shift ϕ is small [*Grant and Madsen*, 1979*b*], and f_e and f_w differ by only 5–10% at most. For a rippled bed, ϕ may approach 45°, and f_e and f_w will differ by more than 5–10%. This difference is not significant when other uncertainties in the data are accounted for, and f_w will be used here interchangeably with f_e. Thus for each experimental run in both Carstens' and Bagnold's studies, the friction factor f_w can be calculated for a given bed condition, i.e., ripples, flat bed, etc.

TABLE 1. Empirical Relationships for Ripple Geometry Under Waves

	Equilibrium Range	Breakoff Range
	$(\psi'/\psi_c) < (\psi'/\psi_c)_B$	$(\psi'/\psi_c) > (\psi'/\psi_c)_B$
η/A_b	$0.22(\psi'/\psi_c)^{-0.16}$	$0.48S_*^{0.8}(\psi'/\psi_c)^{-1.5}$
η/λ	$0.16(\psi'/\psi_c)^{-0.04}$	$0.28S_*^{0.6}(\psi'/\psi_c)^{-1.0}$

Data from W. D. Grant et al. (manuscript in preparation, 1981).

THEORY AND COMPARISON WITH DATA

The total boundary roughness is assumed to be composed of three components: one due to skin friction at the bed, one due to form drag over the wave-formed ripples, and one due to the dissipation associated with a near-bed layer of intense sediment transport. The component due to skin friction at the boundary is at least an order of magnitude smaller than the other two and will be neglected for the conditions of interest here.

Ripple roughness. A dimensional analysis of the turbulent wall layer in a unidirectional shear flow over a rough boundary which considers the role of the relevant length and area scales associated with roughness arrays was carried out by *Wooding et al.* [1973]. A similar analysis is applied here to describe the roughness due to wave-formed ripples. This roughness description is used then to derive an expression for the law-of-the-wall using standard boundary layer scaling arguments. The law-of-the-wall may be expressed in the immediate vicinity of the boundary as

$$u_w/u_{*wm} = F(z/L) \tag{16}$$

where z is the vertical coordinate, positive upward from the bed; u_w is the magnitude of the velocity in the wave boundary layer; u_{*wm} is the characteristic shear velocity given by (6); F is an unknown function; and L is the characteristic length scale for the flow in the surface layer. For a smooth boundary, L is equal to ν/u_* [*Tennekes and Lumley*, 1973]. For a rough boundary, L is related to the geometry of the roughness elements, imposing an additional roughness length. In fully rough turbulent flow, L depends on only the geometry of the roughness elements. The geometrical dependence varies with the roughness type under consideration.

At least three distinct types of roughness configurations exist [*Wooding et al.*, 1973], each with its own scaling law. The first 'k' type roughness [*Perry et al.*, 1969], which is typical of the sand grain roughness studied by *Nikuradse* [1933], is characterized by the formation of unstable eddies behind the roughness elements. These eddies are shed into the flow above the boundary resulting in a turbulence structure scaled to the height of the roughness elements. The 'k' type roughness elements have a spacing between elements of the order of their height or less. The second type, 'δ' type roughness [*Perry et al.*, 1969], is characterized by

the formation of stable eddies between roughness elements which cause 'skimming flow' over the boundary. This type of roughness results in a turbulence structure nearly independent of the roughness height and scaled by u_* and the boundary layer thickness (at least in a zero pressure gradient flow). A third class of roughness, 'k, δ' [*Wooding et al.*, 1973], scales with both the height of the roughness elements and their concentration (concentration is defined as the ratio of the frontal area of each roughness element to the average horizontal surface area). Flow over roughness configurations obeying a 'k, δ' type scaling is characterized by the formation of eddies in the lee of the roughness elements and by the reattachment of the flow between roughness elements. Physically, this behavior requires small concentrations of elements. In addition to the importance of roughness height and concentration, *Wooding et al.* [1973] argue that there is an effect on the flow by the roughness elements which depends on the relative dimensions of their width to height.

Wave-formed ripples obey a roughness law consistent with concentration dependent 'k, δ' roughness. To aid in the development of the appropriate expression for this law, two simplifying assumptions concerning the ripple geometry are possible using laboratory observations of the physical characteristics of wave-formed ripples. First, the ripples may be approximated as two-dimensional roughness elements. Studies by Carstens, Bagnold, and others show that equilibrium ripples are highly two-dimensional. In the breakoff range, three-dimensional effects begin to appear in the form of breaks in the ripple crest, and some misalignment of the crests appears at these breaks. However, the uninterrupted cross-stream crest length is still long in relation to the break width and the ripple wavelength. Second, the width of the ripple crest in the streamwise direction is of the same order as the height of the ripple for typical quartz sand. This width is small in relation to the length of the ripples. Thus the aspect ratio introduced by *Wooding et al.* [1973], which accounts for the width of the roughness element relative to its height, is about 1 and may be neglected. (If the effect of the finite ripple width is significantly underestimated, the expression derived here for the ripple roughness will overpredict the roughness, since a large streamwise ripple width decreases the size of the dissipation eddy behind the ripple.)

Invoking the assumptions of two-dimensionality and an aspect ratio equal to 1, for a fully rough flow over a rippled bed, L will be a function of only the ripple height and the ripple length. Thus L is given by $\eta(\eta/\lambda)$, and the law-of-the-wall becomes

$$u_w/u_{*wm} = F(z/\eta(\eta/\lambda)) \tag{17}$$

where η is the physical roughness scale which makes the fully rough surface hydrodynamically equivalent to other geometrically similar surfaces and η/λ represents the concentration of the roughness elements.

The usual method for determining F in constant-pressure boundary layer flows specifies the velocity defect law for the turbulent outer region of the boundary layer. The outer region is independent of the roughness, and its appropriate scales are the shear velocity and boundary layer thickness. Between the inner region and the outer region of the boundary layer an overlap region exists where the flow characteristics are described by both the outer and inner flow scales [*Clauser*, 1956]. The existence of this overlap region results in the argument that F follows a logarithmic velocity law in the overlap region [*Millikan*, 1939; *Tennekes and Lumley*, 1973]. The determination of F for oscillatory flow is more complicated. The flow in the wave boundary layer is alternatively accelerated and decelerated over a wave period resulting in an additional length scale depending on the ratio of the shear velocity squared to the magnitude of the kinematic pressure gradient [*Yaglom*, 1979]. That is, $\delta_p = u_*^2/|(-1/\rho)\ (\partial p/\partial x)|$ where δ_p is the pressure gradient length scale, u_* is the shear velocity, p is the pressure, and x is the along-stream axis. In smooth wall turbulent shear flows subject to adverse pressure gradients, the usual law-of-the-wall holds at distances from the boundary that are small in comparison to δ_p [*Yaglom*, 1979]. Furthermore, if the overlap layer exists at a distance from the boundary much less than δ_p, the velocity profile is logarithmic.

For smooth wall turbulent shear flows in positive pressure gradients the scaling described above breaks down because of the tendency for the flow to relaminarize [*Yaglom*, 1979]. In contrast, fully rough turbulent shear flows subject to accelerations become rougher [*Coleman et al.*, 1977]. The scaling valid for adverse pressure gradients should be expected to hold for the fully rough positive pressure gradient flows. *Grant and Madsen* [1979*b*] analyzed *Jonsson and Carlsen*'s [1976] rough turbulent wave boundary layer experiments and found the near-bottom velocity profile to be logarithmic over the entire wave period, supporting this argument.

We argue that pressure gradient effects are small near the boundary; then F is logarithmic, and the law-of-the-wall becomes

$$\frac{u_w}{u_{*wm}} = \frac{1}{\kappa} \ln \frac{z}{\beta\eta} + c \tag{18}$$

where β is the roughness concentration and c is a constant. The vaue of c in (18) can be estimated by comparing analogous expressions for the velocity profiles in unidirectional and oscillatory flow. The classical law-of-the-wall for fully rough turbulent unidirectional flow with $z_0 = k_b/30$ applies in the wall region of the wave boundary layer, i.e. [*Grant and Madsen*, 1979*b*],

$$\frac{u_w}{u_{*wm}} = \frac{1}{\kappa} \ln \frac{30z}{k_b} \tag{19}$$

The form of the law-of-the-wall expressed by (18) for waves should be equivalent also to its unidirectional flow counterpart by analogy to the favorable agreement between (19) and unidirectional flow results.

The analogous expression to (18) for unidirectional flow can be found from *Wooding et al.*'s [1973] drag law for fully rough turbulent shear flow in zero pressure gradient over three-dimensional roughness arrays,

$$\frac{U}{u_*} = \frac{1}{\kappa} \ln \frac{\delta}{b\beta'\gamma} - 2.05 \tag{20}$$

where U is the free stream velocity, γ is an aspect ratio to account for the effect of finite width of the roughness

elements in the streamwise direction, β' is the concentration including finite width effects, and b is the height of the roughness elements. The drag law given by (20) is related to the law-of-the-wall for a flat plate in zero pressure gradient through the velocity defect law

$$\frac{u - U}{u_*} = \frac{1}{\kappa} \ln \frac{z}{\delta} + 2.25 \tag{21}$$

where δ is the boundary layer thickness. Substituting (20) into (21) results in the expression for the law-of-the-wall

$$\frac{u}{u_*} = \frac{1}{\kappa} \ln \frac{z}{b\beta'\gamma} + 0.2 \tag{22}$$

The constant 0.2 in (22) is independent of any assumptions concerning the outer flow region. Differences in the value of von Karman's constant associated with the additive constants in (20) and (21) have been ignored in the manipulation leading to (22). Thus the value 0.2 for the constant in (22) is an estimate only, whose accuracy will be determined through data comparisons. Equating (18) and (22) and noting that for wave-formed ripples, γ is unity and b equals η, c in (18) is equal to 0.2.

Equations (19) and (18) with c equal to 0.2 represent two expressions for the law-of-the-wall valid in the wave boundary layer; the latter expression explicitly includes the influence of the relevant geometrical length and area scales on the inner layer velocity profile, whereas these scales are implicit in k_b in (19). By equating (18) and (19), k_b may be expressed in terms of the geometry of the wave-formed ripples as

$$k_b = 27.7(\eta)(\eta/\lambda) \tag{23}$$

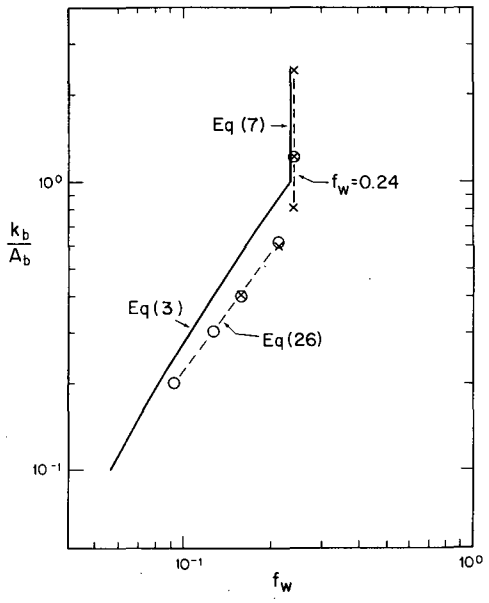

Fig. 2. Comparison between *Bagnold*'s [1946] experimentally determined friction factors and the theoretically predicted friction factor from (23), (3), and (7). Two ripple lengths of 10 cm (circles) and 20 cm (crosses) were used with a fixed steepness of ~0.15. The range of k_b/A_b between 0.6 and 1 corresponds to natural ripple steepnesses. Note that for $k_b/A_b > 1$, f_w equals a constant.

Comparison of the ripple roughness with data and other theories. Predictions of friction coefficients using (23) to determine the equivalent roughness heights can be compared with results from Bagnold's experiments. For the ripple geometry used in Bagnold's experiments, (23) can be rewritten in dimensionless form as

$$k_b/A_b = 4.13\eta/R \tag{24}$$

where the imposed oscillation amplitude of the rippled plate, R, in Bagnold's experiment is equivalent to the characteristic length scale for the wave motion at the bed, A_b. For $R/\lambda > 1$, Bagnold determined an empirical relationship between the drag coefficient calculated for each run and the corresponding value of R/λ. Noting that Bagnold's drag coefficient is equal to $f_w/3$, his empirical expression may be rewritten in terms of f_w as

$$f_w = 0.216(R/\lambda)^{-0.75} \tag{25}$$

and (24) and (25) may be combined to yield an expression for f_w in terms of the relative roughness which can be compared directly with (3) since $\eta/R = 0.15\lambda/R$ in Bagnold's experiment. Thus for $R/\lambda > 1$, Bagnold's experiments give

$$f_w = 0.31(k_b/A_b)^{3/4} \tag{26}$$

For $R/\lambda < 1$, Bagnold found that his drag coefficient was a constant corresponding to $f_w = 0.24$.

When the relative roughness is calculated from (24), values of f_w predicted using (3) and (7) show reasonable agreement with those determined from Bagnold's experiments (Figure 2). For values of $R/\lambda > 1$, f_w calculated from (3) is 10–20% smaller than f_w given by (26). For values of $R/\lambda < 1$, the values of f_w predicted from (7) are in close agreement with Bagnold's experimental values of 0.24. The arguments leading to (23) were made for natural ripples. Improper scaling of Bagnold's artificial ripples relative to natural ripples may explain the differences between (3) and (26) for experiments in which $R/\lambda > 1$.

For natural ripples, as the excursion amplitude exceeds the ripple spacing, ripple height decreases. In Bagnold's experiments, where $R/\lambda > 1$, a corresponding decrease in ripple height does not occur as R/λ increases, since the steepness is fixed. As a result, the internal boundary layer developed over the ripple crest does not reattach, providing little contribution to the total shear stress from skin friction over the ripple surface. Bagnold's description of the flow behavior over the ripples at large values of R/λ supports this picture; small unstable eddies develop in the ripple trough, which are shed into the flow. This type of eddy shedding favors a roughness which scales more with height of the elements and less with concentration [cf. *Perry et al.*, 1969]. If this is true, the roughness model given by (24) would be expected to underpredict the roughness, as is observed.

The experimentally determined friction coefficient from Carstens' experiments is plotted in Figure 3 as a function of the relative roughness in which k_b is determined from the observed ripple geometry using (23). The relationship given by (3) and (7) for the friction factor is plotted for comparison. Close agreement between the theory and data occurs for $k_b/A_b > 0.3$. Use of (23) consistently underpredicts f_w for values of $k_b/A_b < 0.3$.

A summary (Table 2) of the experimental points from Carstens' study shows for values of $k_b/A_b > 0.3$ that the bed

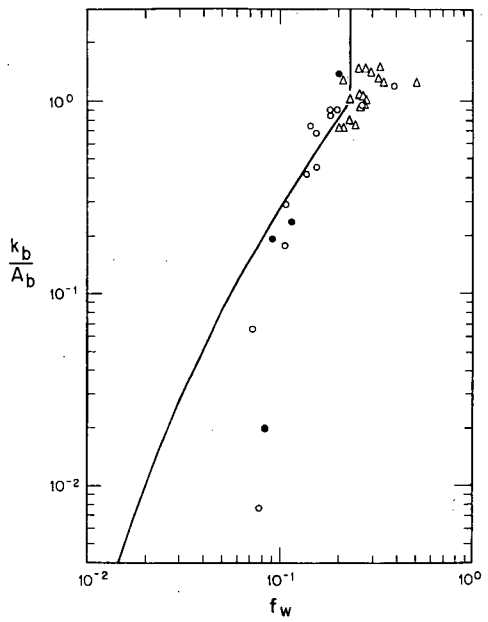

Fig. 3. Results of *Carstens et al.*'s [1969] experiments with k_b determined from (23) and f_w determined experimentally. The solid curve is the friction factor equation given by (3) and (7); for open circles, $d = 0.0297$ cm; for solid circles, $d = 0.019$ cm; and for triangles, $d = 0.0585$ cm. See Table 1 for more details.

contains ripples in the equilibrium range (i.e., $(\psi'/\psi_c) < (\psi'/\psi_c)_B$ in the table). In this range, large form drag and low values of sediment transport are expected. Equation (23) successfully accounts for most of the dissipation in this range of relative roughness. At the other extreme, for $k_b/A_b < 0.1$, the bed is nearly flat, $(\psi'/\psi_c) > (\psi'/\psi_c)_B$, and the sediment transport rate is large. Differences between the ripple roughness model and the experimental results for $k_b/A_b < 0.3$ are discussed in the next section.

The theory developed here predicts that k_b is directly proportional to the ripple height and concentration. Models with a similar dependence have been proposed by *Lettau* [1969] for the aerodynamic roughness in atmospheric boundary layer flows, $k_b = 15\eta \cdot \eta/\lambda$, and by *Swart* [1977] for waves, $k_b = 25\eta \cdot \eta/\lambda$. Swart's expression is based entirely on empirical correlations and does not include either Bagnold's or Carstens' data. *Arya* [1975] developed a more complicated relationship for the roughness length as a function of roughness element height, shape, slenderness, concentration, and the roughness of the intervening surface between elements. This latter theory is limited to concentrations small in relation to typical wave-formed ripple concentrations.

The effect of near-bed sediment transport on k_b. The underprediction of the friction factor for Carstens' experiments where the relative roughness is less than 0.3 and k_b is calculated from (23) is evidence of a larger dissipation in the flow than that due to form drag. For a relative roughness less than 0.1 the bed was nearly flat (Table 2). Neglecting sediment transport effects, the sand grain diameter would be the appropriate roughness in such a fully rough turbulent flow. However, calculations of dissipation based on the sand grain diameter are an order of magnitude smaller than the observed dissipation.

Qualitatively, the arguments of *Owen* [1964] for the effect of sediment transport on aeolian flows give a plausible reason for the behavior exhibited in Figure 3. *Owen* [1964] hypothesized that the turbulence within the saltation layer is associated with the wake structure caused by the movement of the sediment grains relative to the surrounding fluid. The concentration of particles in the near-bed sediment transporting layer is governed by the requirement that the shear stress distribution within the layer varies from a maximum at the top to the critical stress for initiation of motion at the bed. As the shear stress above the layer increases, the sediment concentration in the layer increases so as to maintain the critical shear stress at the bed, increasing the roughness associated with the layer. The divergence between the data and theory in Figure 3 increases with increasing sediment transport (see Table 2) and is consistent with the behavior expected from Owen's model.

The roughness associated with the layer of intense near-bed sediment transport is proportional to the thickness of the layer according to *Owen*'s [1964] hypothesis. Thus an appropriate expression for the thickness of the near-bed sediment transporting layer is needed to apply Owen's hypothesis. In

TABLE 2. Data From Carstens' Experiments Plotted in Figures 3 and 4

Run	$k_b(23)/A_b$	f_w	η/λ	ψ'/ψ_c	$(\psi'/\psi_c)/(\psi'/\psi_c)_B$
		$d = 0.0297$ cm; $s = 2.47$			
21	0.962	0.263	0.171	1.09	0.22
22	0.894	0.198	0.175	1.61	0.33
23	0.900	0.181	0.176	2.03	0.41
24	0.837	0.184	0.179	2.41	0.49
25	0.745	0.144	0.170	4.10	0.83
26	0.688	0.152	0.162	4.97	1.01
27	0.449	0.154	0.132	6.06	1.23
29B	0.296	0.105	0.115	8.45	1.72
30B	0.177	0.106	0.106	10.19	2.07
31B	0.008	0.077	0.026	15.16	3.08
32B	0.066	0.072	0.065	11.90	2.42
36	0.416	0.137	0.131	6.74	1.37
51	1.200	0.391	0.183	0.91	0.18
		$d = 0.0585$ cm; $s = 2.62$			
63	1.460	0.255	0.191	0.89	0.09
64	1.450	0.278	0.195	1.19	0.13
65A	1.250	0.341	0.186	1.48	0.16
66	1.300	0.321	0.193	1.91	0.20
67	1.288	0.210	0.190	2.42	0.26
68	1.500	0.328	0.206	2.64	0.28
69	1.411	0.294	0.200	3.30	0.35
70	1.00	0.277	0.185	3.77	0.40
71	1.00	0.271	0.185	3.96	0.42
72	1.075	0.254	0.187	4.48	0.47
73	0.913	0.257	0.192	5.19	0.55
74	1.045	0.257	0.197	5.58	0.59
75	0.740	0.244	0.150	6.24	0.66
76	0.981	0.225	0.181	7.14	0.76
77	0.782	0.226	0.173	7.84	0.83
78	0.716	0.202	0.148	8.49	0.90
79	0.710	0.200	0.157	9.67	1.02
80A	1.240	0.517	0.180	1.25	0.13
		$d = 0.019$ cm; $s = 2.66$			
106A	0.237	0.115	0.106	3.27	0.96
111A	0.193	0.920	0.125	4.97	1.47
112B	0.020	0.085	0.048	7.63	2.25
114A	1.408	0.200	0.199	1.04	0.31

The run numbers correspond to data from Tables I–XII of *Carstens et al.* [1969]; k_b (23) is calculated using (23); and $(\psi'/\psi_c)_B$ is calculated from (8).

oscillatory flows the fluid forces acting on a sediment grain vary over a wave cycle, and the maximum resuspension of sediment occurs at approximately the maximum shear stress; this is also the time of maximum dissipation. The maximum thickness of the layer is a logical choice to relate the roughness to in the case of oscillatory flows.

To estimate the scale of the saltation layer thickness, we follow *Owen* [1964] and take the vertical momentum equation for a sediment particle

$$(\rho_s + \rho C_m)V \frac{\partial^2 z}{\partial t^2} + (\rho_s - \rho)Vg + F_D = 0 \qquad (27)$$

in which V is the volume of the sediment particle, F_D is the vertical component of the drag force, and since the fluid is water, the effect of added mass has been included through the added mass coefficient C_m. Linearizing the drag force in the form

$$F_D = KV\,(\partial z/\partial t) \qquad (28)$$

as did Owen, the resulting equation reads

$$\frac{\partial^2 z}{\partial t^2} + \frac{K}{\rho(s + C_m)} \frac{\partial z}{\partial t} + \frac{s - 1}{s + C_m} g = 0 \qquad (29)$$

which is subject to the initial conditions of $z = 0$ and $\partial z/\partial t = v_i$, equal to the initial vertical velocity at $t = 0$.

This equation is readily solved as done by *Owen* [1964], who chose $K = \rho(s - 1)g/w$, where w is the fall velocity of the particle. Upon expanding his solution in the assumed small parameter v_i/w and retaining only the leading terms, Owen's solution is identical to the solution obtained from (27) and (29) if the drag force is neglected from the outset. This approach is equivalent to a balance between the initial kinetic energy of the particle and the potential energy when the particle is at its highest elevation and leads to a conservative but simple relationship for h_t, the maximum jump height,

$$h_t \leq \frac{(s + C_m)}{(s - 1)} \frac{v_i^2}{2g} \qquad (30)$$

To use (30), we approximate the particles as spheres ($C_m = 1/2$), and the all-important quantity becomes the initial vertical particle velocity. In the immediate vicinity of a flat bed the limiting value for v_i is the maximum horizontal particle velocity. A reasonable physical mechanism which converts the particle horizontal velocity to a vertical velocity is through collisions with stationary particles on the bed. Particles leaving the bed with a vertical velocity equal to their horizontal velocity determine the maximum height of the layer.

The magnitude of the maximum horizontal velocity of a particle subject to the action of surface gravity waves can be calculated by considering a balance of the maximum horizontal forces acting on it. The time required for a sediment particle to accelerate from zero velocity to 90% of its maximum horizontal velocity is $O(d/u_{*wm})$ (see appendix). For strong transporting conditions this time is $O(10^{-2})$ s. Thus in the following analysis, no significant variation in the fluid forces acting on the particle is assumed to occur during the time the particle is accelerating. This acceleration time scale is much less than the time required for a particle to return to the bed from the top of the near-bed transport layer, so it can be expected that particles will reach this velocity. The balance of horizontal forces on the particle will consist of a friction force, a drag force in phase with the fluid velocity, and an inertia force in phase with the fluid acceleration. Particle concentrations are assumed to be small ($<10^{-3}$), and therefore particle-particle interactions are neglected.

The maximum resultant force due to the drag and inertia forces depends on the relative magnitude of the maxima of the two forces:

$$F_{em} = \left[1 + \left(\frac{F_{IM}}{2F_{DM}}\right)^2\right] F_{DM} \qquad F_{IM} < 2F_{DM} \qquad (31)$$

$$F_{em} = F_{IM} \qquad F_{IM} > 2F_{DM} \qquad (32)$$

where F_{em} is the maximum resultant force, F_{IM} is the maximum inertia force

$$F_{IM} = (1 + 1/2)V\rho\omega e u_{*wm}' \qquad (33)$$

for a spherical particle, and F_{DM} is the maximum drag force

$$F_{DM} = \tfrac{1}{2}\rho C_D (e u_{*wm}')^2 A \qquad (34)$$

where V is the volume of the particle, A is the cross-sectional area of the particle, C_D is the drag coefficient, eu_{*wm}' is the fluid velocity in the near-bed sediment transport layer where the appropriate roughness is the grain diameter, e is a proportionality constant, and u_{*wm}' is given by (6). Equation 34) can be rewritten as

$$F_{DM} = \left(\tfrac{1}{2} C_D \frac{\pi}{4} d^2 e^2\right) \tau_{bm}' \qquad (35)$$

Using (10), the ratio F_{IM} to F_{DM} becomes

$$\frac{F_{IM}}{F_{DM}} = \frac{2(2)^{1/2}}{C_D\, e (f_w')^{1/2} (A_b/d)}$$

Anticipating the results below, e is taken as 9.2, and for typical conditions, $C_D = 0.4$, $f_w' \sim O(10^{-2})$, and $A_b/d \sim (10^3)$. Hence $F_{IM}/F_{DM} << 1$, and the maximum resultant force is given approximately by the drag force.

The horizontal balance of maximum forces can be expressed as

$$\left[\frac{\pi}{6} d^3 \rho g(s - 1) - \tfrac{1}{2}\rho C_L (e u_{*wm}' - u_p)^2 \frac{\pi}{4} d^2\right] \tan \phi$$

$$= \frac{\pi}{4} d^2 \tfrac{1}{2} \rho C_D (e u_{*wm}' - u_p)^2 \qquad (37)$$

where the term on the left-hand side is the friction force for he particle moving along the bed and is composed of the submerged weight of the particle and the lift force on the particle, respectively. C_L is the lift coefficient, and ϕ is the friction angle. The term $(eu_{*wm}' - u_p)$ is a relative fluid velocity, since u_p is the particle velocity. Solving (37) for u_p yields

$$u_p = e u_{*wm}' - \left[\frac{dg(s -) \tan \phi}{\frac{3}{4}(C_D + C_L \tan \phi)}\right]^{1/2} \qquad (38)$$

At initiation of motion the force balance given by (37) holds if the relative fluid velocity is replaced by $e_c u_{*c}'$ where e_c is a proportionality constant and u_{*c}' is the critical shear veloci-

ty for initiation of sediment motion. The second term on the right-hand side of (38) is simply ($e_c u_{*c}'$) assuming that the lift and drag coefficients in (38) are the same as those for initiation of motion. The particle velocity is then

$$u_p = e u_{*c}' \left[\frac{u_{*wm}'}{u_{*c}'} - b \right] \tag{39}$$

where $b = e_c/e$. Equation (39) can be expressed in terms of Shields' parameter as

$$u_p = e[(s - 1)gd]^{1/2} \psi_c^{1/2} [(\psi'/\psi_c)^{1/2} - b] \tag{40}$$

Since the response time of sediment particles to turbulent fluctuations is rapid in relation to the time scale for waves, the instantaneous response of the particles under waves is most likely similar to that in unidirectional flow. *Madsen and Grant* [1976] have demonstrated the reasonable nature of this hypothesis, provided that the shear stress under the wave is correctly determined. Adopting the above hypothesis, the experiments of *Luque and Beek* [1976] can be used to determine the coefficients e and b. *Kobayashi* [1979] found $e = 9.2$ and $b = 0.7$ using these experiments, in an analysis for unidirectional flow. The exact value of these coefficients may vary, but it is likely that the values given above are reasonable estimates.

The maximum thickness of the near-bed transport layer is found using (40) and (30) with $C_m = 1/2$ as

$$h_t = (e^2/2)\ (s + 1/2) d\psi_c[(\psi'/\psi_c)^{1/2} - b]^2 \tag{41}$$

Owen's [1964] hypothesis assumes $z_0 = \alpha_0 h_t$. The value of α_0 can be determined from Carstens' data. Since even for large sediment–transporting situations the bed was not exactly planar (showing ripple slopes of 0.1–0.02), a correction must be made for the contribution of the form drag to the total drag associated with the dissipation calculated in the experiments. In an effort to minimize dependence of α_0 on the model used to correct for the form drag, only runs where the ratio $(\psi'/\psi_c)/(\psi'/\psi_c)_B$ was greater than 2 were used (see Table 2). For these runs, the form drag roughness calculated from (23) ranged from ~50 to 5% of the total roughness. The total roughness was defined as the value required to make the experimental value of f_w match the predicted value using (3). The parameter α_0 was found to have an average value equal to 0.13.

The contribution to the total roughness of the near-bed sediment transport is then

$$k_{bs} = 3.8(e^2/2)(s + C_m) d\psi_c[(\psi'/\psi_c)^{1/2} - b]^2 \tag{42}$$

Inserting the values for e and b,

$$k_{bs} = 160(s + C_m) d\psi_c[(\psi'/\psi_c)^{1/2} - 0.7]^2 \tag{43}$$

where $z_0 = k_{bs}/30$.

Comparison of the sediment transport roughness with other theories. The primary difference between the analysis in the previous section and the approach used by *Smith and McLean* [1977] for the 'bed load' roughness in unidirectional flow is the estimate of the initial sediment velocity.

Smith and McLean [1977] argued that the initial kinetic energy of a sediment particle is equal to the work done in removing the particle from the bed. The work done is equal to the excess friction at the bed times the cross-sectional area of the particle times the distance over which the particle accelerates. For waves this results in an initial velocity v_i proportional to

$$v_i \propto \left(\frac{\tau_{bm}' - \tau_c}{\rho_s} \right)^{1/2} \tag{44}$$

where τ_c is the critical shear stress under the wave for initiation of motion. Letting $C_m = 1/2$ and letting v_i be given by (44), the thickness of the bed load layer can be obtained from (30):

$$h_t \propto \frac{d(s + 1/2)}{2s} \psi_c[\psi'/\psi_c - 1] \tag{45}$$

The same procedures used to determine α_0 in (41) applied to (45) give α_0 equal to 27.6 and

$$k_{bs} = 827 \frac{d(s + 1/2)}{2s} \psi_c[\psi'/\psi_c - 1] \tag{46}$$

A comparison of (45) and (41) shows the similarity of the two expressions for high values of ψ'/ψ_c, which is the case of interest here. The major difference is in the dependency on the relative sediment density and the inclusion of the proportionality constant e. For quartz sand in water, $s = 2.65$ and the factor $(s + 1/2)/2s$ can be lumped with α_0, allowing a comparison of the results for waves with *Smith and McLean*'s [1977] Columbia River results. These results and the results of (43) are summarized in Table 3. In the wave model given by (46), h_t is the maximum value theoretically expected during the accelerating phase of the flow. The lower value of the coefficient in Table 3 for the waves, as compared to the steady flow result, may represent the effect of an overprediction of the average dissipation due to using the maximum thickness for h_t. Therefore the fact that the ratio is in the range of one half is not surprising.

Carstens' experiments indicate that z_0 is 7–8 grain diameters for experiments at high transport conditions. For the same conditions the ratio of h_t/d is 23–53 diameters using h_t

TABLE 3. Relationships for z_0 Due to Near-Bed Sediment Transport for Oscillatory Flow (Equations (43) and (46)) and Unidirectional Flow

k_{bs}	z_{0s} ($s = 2.65$)	h_t/d*	z_{0s}/h_t	Comment
(43)	$17d\psi_c[(\psi'/\psi_c)^{1/2} - 0.7]^2$	23–53 (41)†	0.13	v_i given by (40)
(46)	$16.5d\psi_c[\psi'/\psi_c - 1]$	0.1–0.3 (45)	28	Modification of *Smith and McLean* [1977] oscillatory flow; v_i given by (44)
Smith and McLean [1977]	$26.3d\psi_c[\psi'/\psi_c - 1]$			v_i (based on lift in steady flow)

*Values of h_t/d for range of ψ'/ψ_c from 8 to 15 with $d = 0.03$ cm.
†Number in parentheses indicates equation number for h_t or v_i.

given by (41). To the authors' knowledge, z_0 always lies within the roughness elements or in the case of smooth turbulent flow is always less than the sublayer thickness. The ratio of z_{0s}/h_t corresponding to (43) is approximately 0.13, satisfying this observation. The same parameters corresponding to (46) are listed in Table 3 and demonstrate the less realistic result of $h_t < d$ and $z_{0s} > h_t$. It should be recalled that h_t given by (45) is expected to represent only the scale of the near-bed sediment transporting layer rather than its actual magnitude so this difference is not of great practical importance. What is of importance is that the approach for waves yields results comparable to the unidirectional flow results, despite the fact that different data sets were used in the determination of α_0. This appears particularly important for the case of waves where only four data points were available for the determination of α_0. Thus the favorable comparison between the present results and those of *Smith and McLean* [1977] lends credibility to the expression for the roughness given by (43).

Combined roughness model. The total roughness under the wave is the sum of the form drag component (equation (23)) and the sediment transport component (equation (43)). The relative roughness is then

$$\frac{k_b}{A_b} = 160(s + C_m)\frac{d}{A_b}\psi_c[(\psi'/\psi_c)^{1/2} - 0.7]^2 + 28\frac{\eta}{A_b}\frac{\eta}{\lambda} \quad (47)$$

The sediment transport component given by (43) was favored in (47) because of the physically reasonable behavior of z_0 and h_t (Table 3). The lack of an independent data set and the limited data of Carstens prevent a more definitive test of the model. Clearly, (46) also fits Carstens' data and follows a close physical analogy with *Smith and McLean*'s [1977] Columbia River results.

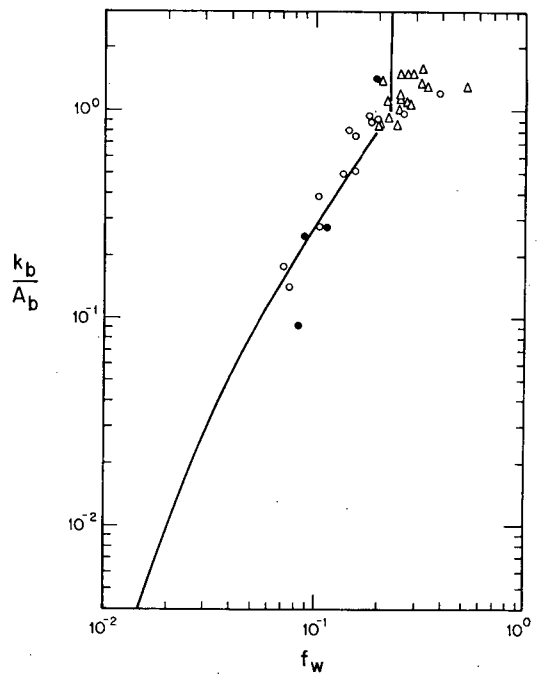

Fig. 4. *Carstens et al.*'s [1969] experiments with k_b/A_b determined from (47) and f_w determined experimentally. Solid curve is the wave friction factor equation given by (3) and (7). See Figure 3 for comparison and explanation of symbols.

The assumption that the roughness associated with the form drag can be added to the roughness associated with the sediment transport does not greatly affect the results. Ripples tend to dominate the roughness when they are present. At high boundary shear stresses relative to the critical stress the sediment transport dominates the roughness, but the ripples are of small steepness in this range. Figure 4 compares Carstens' data with the theoretically predicted friction factor using (47) to evaluate the relative roughness.

IMPLICATION OF RESULTS FOR CONTINENTAL SHELF FLOWS

The total friction over a movable bed under waves can be calculated using (47) and (3) or (7). Evaluation of the parameters in (48) is straightforward. The ψ_c can be determined from Shields' curve [*Madsen and Grant*, 1976], and ψ' can be evaluated using (14) with the relative roughness based on d/A_b. The critical shear stress on a quartz sand bed with a negative slope angle equal to the angle of repose of the sediment is only 40% greater than the flat bed value [*Luque and Beek*, 1976]. Thus errors associated with using flat bed values of ψ_c when ripples are present are of the same magnitude as the scatter in Shields' diagram and the effect of bioturbation. The parameters η and η/λ are best determined from bottom observations. If no observations are available, they may be predicted from empirical relationships relating ripple height and steepness to the boundary shear stress (e.g., W. D. Grant et al., manuscript in preparation, 1981, and Table 1, this paper; or other existing empirical relationships). The field data base for wave-formed ripples is sparse, and caution must be exercised in applying empirical relationships.

The flow on the middle and inner continental shelf generally will consist of both surface waves and currents. In principle, (47) can be used to calculate the roughness for this case. Evaluation of the parameters described above must be done using the total boundary shear stress which can be calculated using the model of either *Grant and Madsen* [1979*a*] or *Smith* [1977]. The boundary shear stress will be enhanced because of the combined flow, and the flat bed condition will occur under milder wave conditions. For strong wind forcing, the bed often will be flat or nearly so, and most of the roughness contribution is associated with the sediment transport term in (47).

The roughness for the flow inside the wave boundary layer is predicted by (47). Outside the wave boundary layer the primary effect on the current is an increased or apparent roughness due to the influence of the waves, as described by *Grant and Madsen* [1979*a*, *b*]. To predict this apparent roughness, knowledge of the roughness inside the wave boundary layer is required. The value of α_0 in (47) should approach the steady flow value when the magnitude of the wave orbital velocity, u_{bm}, approaches the magnitude of the current inside the wave boundary layer. The steady flow value must be determined from data if the model given in (47) is to be used with high accuracy. A reasonable estimate for the steady flow value of α_0 would be about twice the oscillatory flow value on the basis of the comparison given above between the steady flow and oscillatory flow analysis using *Smith and McLean*'s [1977] approach.

Reasonable order of magnitude estimates of the roughness for the combined flow case should result from the approach

described above. Logarithmic velocity profiles are not highly sensitive to small errors in the roughness. Estimates of boundary shear stress using (1) are more sensitive to roughness estimates for a large relative roughness, and predictions of boundary shear stress should have appropriate error bars included with them. Factor of 2 error bars on the roughness estimate will not severely affect the calculation of mean current velocity profiles for the combined flow case. The bottom roughness is often used as an adjustable parameter when fitting a logarithmic profile to near-bottom flow measurements. For neutral stratification, three other parameters are involved in specifying the log profile: the shear velocity, the origin of the theoretical bed level, and von Karman's constant. The independent specification of z_0 is an important step in understanding the behavior of the other parameters.

Estimates of dissipation of wave energy by bottom friction are greatly influenced by the inclusion of the effect of bed load transport in the roughness experienced by the wave. The value of the relative roughness over a flat bed generally is taken as $k_b = d$ whether or not sediment transport is occurring. A friction factor of order 10^{-2} is predicted for typical sand grain diameters and wave conditions. Inclusion of the sediment transport effect shows that the value of the friction coefficient should be of order 10^{-1} for the flat bed at high shear stresses. This point is supported by Carstens' results plotted in Figures 3 and 4, where the value of the friction factor is determined directly from the data with no assumptions concerning the roughness. Most attempts to attribute changes in wave conditions between two points to frictional dissipation have not been successful. The typical value taken for f_w in dissipation models is 0.02, corresponding to the grain roughness [e.g., *Bretschneider*, 1959; *Hasselman and Collins*, 1968]. The results here indicate that over sand beds, friction factor estimates of 0.02 are low by a factor of 5–10. The low friction factor estimates are often offset by a compensating error. Estimates of wave dissipation in the field are usually made for conditions where relatively small currents are present, as well as the wave [e.g., *Shemdin et al.*, 1977]. In these cases the velocity used in the quadratic drag law is the sum of the wave and current velocities. The combined wave and current model of *Grant and Madsen* [1979*a*, *b*] shows that for large waves and small currents the wave friction factor and the wave-current friction factor are approximately the same. Furthermore, the current has little effect on the wave, and the friction associated with the wave dissipation is quadratic in u_b only. With these points in mind, the value of the friction factor predicted here and the values inferred from various field measurements of wave dissipation reported by *Shemdin et al.* [1977] are in reasonable agreement.

SUMMARY AND CONCLUSIONS

A model to compute the roughness for oscillatory flow over a movable bed is presented. The roughness is divided into contributions due to the form drag over wave-formed ripples and the near-bed sediment transport. The roughness is found to be described by a stress dependent function, as is the case for the analogous steady flow problem treated by *Smith and McLean* [1977]. The form drag contribution is derived using standard unidirectional flow scaling analysis. Determination of a roughness function which depends on the ripple height and steepness follows from an analogy with unidirectional flow results. Comparison of the expression with data for artificial ripples and natural ripples in oscillatory flow shows good agreement. The results demonstrate that when ripples having steepnesses greater than 0.1 are present, they determine the majority of the magnitude of the roughness under the waves.

For ripple steepnesses less than about 0.1 under high sediment transport conditions, the roughness depends to a large extent (or for a flat bed, totally) on the intensity of the near-bed sediment transport. The layer of sediment particles contributing to this roughness is of the order of 7–8 grain diameters in Carstens' experiments. Following *Owen*'s [1964] hypothesis, the roughness associated with the near-bed sediment transport is related to the thickness of the layer. For high sediment transport rates over a flat bed the order of magnitude of z_0 is well predicted using an initial vertical particle velocity equal to the maximum horizontal velocity of the particle and a scale estimate for the layer thickness based on conservation of energy arguments. The model assumes that particles moving horizontally over the bed are deflected upward through collisions with particles resting on the bed. The maximum horizontal particle velocity is calculated assuming that the drag and lift forces on the particle are based on the relative velocity $(eu_{*wm}' - u_p)$. The value of e is determined from steady flow experiments. This value is argued to be a good estimate of the magnitude of e even in oscillatory flow, since the particle response time is found to be much faster than the time scale of any significant changes in the forces on the particle. The parameter z_0 is related to the layer thickness using Carstens' data. The results of the model are physically reasonable and agree well with available data on purely oscillatory flows. More data are needed to make definitive tests of the model predictions, however.

The model for the bottom roughness is easily incorporated into the combined wave and current models of either *Grant and Madsen* [1979*a*, *b*] or *Smith* [1977]. The model is applicable to wave-dominated conditions; this is not felt to be a severe limitation, since relatively large waves and small currents are the expected case for the middle and inner shelf under moderate winds and for most of the shelf under strong winds (it is important to keep in mind that wave-dominated is used in the sense defined by *Grant and Madsen* [1979*a*, *b*]; i.e., the ratio of the near-bottom orbital wave velocity to the current velocity inside the wave boundary layer is order 1 or greater).

A direct test of the model cannot be made for combined wave and current flows because of lack of data. Arguments are made to suggest that the results should be reasonable. It is encouraging that the analysis for waves given here agrees closely with *Smith and McLean*'s [1977] unidirectional flow results.

A nearly flat bed with a high sediment transport rate is a condition that can be expected over much of the inner and middle shelf during storms. On the basis of the results presented here, commonly used estimates of the friction coefficient are a factor of 5–10 too low for these cases. This has important implications on wave dissipation estimates.

The experimental data and the model presented here, along with *Smith and McLean*'s [1977] work, indicate that knowledge of the effects of sediment transport on the near-bottom flow field may be important for most conditions typical of the continental shelf. As a result, hydrodynamic

models employing a constant friction factor or a constant bottom roughness must be used with caution in situations where sediment transport may occur.

APPENDIX

To show that the response time of a sediment particle on the bottom is short in relation to the time scale of a wave motion, we consider the special case of a spherical bottom particle experiencing the fluid force associated with a sudden increase in fluid velocity from $U = 0$ to $U = U$ at $t = 0$. The appropriate form of the governing equation is for this case

$$\rho(s + \tfrac{1}{2})V \frac{\partial u_p}{\partial t} = \tfrac{1}{2}\rho C_D A(U - u_p)^2 - F_f \qquad \text{(A1)}$$

in which u_p is the particle velocity and F_f represents the frictional force between the bottom and the particle.

Introducing the relative velocity

$$u_r = U - u_p \qquad \text{(A2)}$$

and taking $u_{r\infty} = u_r$ as $t \to \infty$ when acceleration is negligible, we have

$$u_{r\infty} = [F_f/(\tfrac{1}{2}\rho C_D A)]^{1/2} \qquad \text{(A3)}$$

With these assumptions, (A1) may be written

$$-\frac{du_r}{dt} = \frac{3}{4}\frac{C_D}{s + 1/2}\frac{1}{d}(u_r^2 - u_{r\infty}^2) \qquad \text{(A4)}$$

Assuming C_D = const, this equation is readily solved subject to the initial condition of $u_r = U$ at $t = 0$. The solution is

$$\frac{3}{4}\frac{C_D}{(s + 1/2)d}t = \frac{1}{2u_{r\infty}}\ln\left\{\frac{u_r + u_{r\infty}}{U + u_{r\infty}}\frac{U - u_{r\infty}}{u_r - u_{r\infty}}\right\} \qquad \text{(A5)}$$

Taking as a measure of the particle response time the time required for the particle to reach 90% of its steady state velocity, $u_{p\infty}$, we obtain from (A5)

$$\frac{3}{4}\frac{C_D}{(s + 1/2)d}t_{90} = \frac{1}{2u_{r\infty}}\ln\left\{\frac{(2u_{r\infty} + 0.1u_{p\infty})}{(U + u_{r\infty})}\frac{(U - u_{r\infty})}{(0.1u_{p\infty})}\right\} \qquad \text{(A6)}$$

From the steady state analysis carried out in the main text we have from (39) and (40)

$$u_{p\infty} = eu_{*wm}' - e_c u_{*c}' = U - U_c \qquad \text{(A7)}$$

where $U_c = e_c u_{*c}'$ is the critical velocity to initiate motion. Since our interest is in flows of high transport corresponding to $U_c << U$, (A6) may be written in the approximate form

$$\frac{3}{4}\frac{C_D}{(s + 1/2)d}t_{90} = \frac{1}{2U_c}\ln\left(1 + 18\frac{U_c}{U}\right) \qquad \text{(A8)}$$

As an upper limit we may take $U_c/U \leq 0.4$ to obtain

$$t_{90} \leq \frac{4}{3}\frac{s + 1/2}{C_D e_c}\frac{d}{u_{*c}'} \simeq \frac{d}{u_{*c}'} \qquad \text{(A9)}$$

when $C_D = 0.4$, $e_c \simeq O(10)$, and $s = 2.65$.

To obtain a typical value for t_{90}, we rewrite (A9) in terms of the critical Shields' parameter ψ_c, which is of the order of 0.05, to obtain

$$t_{90} \simeq (\psi_c(s - 1))^{1/2}\left(\frac{d}{g}\right)^{1/2} \simeq 3.5\left(\frac{d}{g}\right)^{1/2} \qquad \text{(A10)}$$

for quartz in water. For $d \leq 0.1$ mm, (A10) shows the typical response time to be of the order of 10^{-2} s, i.e., much shorter than the time scale of the wave motion.

Acknowledgments. The research described in this paper was supported under NOAA sea grant NA79AA-D-00102 and NA79AA-D-00101 and National Science Foundation grant OCE77-25958. We also thank T. A. Stefanick for assistance in the data reduction and G. McManamin and A. Sousa for typing the manuscript. Contribution 4688 from Woods Hole Oceanographic Institution.

REFERENCES

Arya, S. P. S., A drag partition theory for determining the large-scale roughness parameter and wind stress on the Arctic pack ice, *J. Geophys. Res., 80*(24), 3447–3454, 1975.

Bagnold, R. A., Motions of waves in shallow water; interaction between waves and sand bottom, *Proc. R. Soc. London, Ser. A, 185*, 1–15, 1946.

Bretschneider, C. L., Wave variability and wave spectra for wind generated gravity waves, *Tech. Memo. 118*, U.S. Army Corps of Eng., Beach Erosion Board, 1959.

Carstens, M. R., R. M. Neilson, and H. D. Altinbilek, Bed forms generated in the laboratory under oscillatory flow: Analytical and experimental study, *Tech. Memo. 28*, U.S. Army Corps of Eng., Coastal Eng. Res. Center, June 1969.

Clauser, F. H., The turbulent boundary layer, in *Advances in Applied Mechanics*, vol. 4, edited by H. C. Dryden and J. von Karman, pp. 1–51, Academic, New York, 1956.

Coleman, H. W., R. J. Moffat, and W. M. Kays, The accelerated fully rough turbulent boundary layer, *J. Fluid Mech., 82*, 507–528, 1977.

Dyer, K. R., Velocity profiles over a rippled bed and the threshold of movement of sand, *Estuarine Coastal Mar. Sci., 10*, 181–199, 1980.

Grant, W. D., Oscillatory boundary layers: A comparison between theory and experiment, internal report, Woods Hole Oceanogr., Inst., Woods Hole, Mass., 1980.

Grant, W. D., and O. S. Madsen, Combined wave and current interaction with a rough botom, *J. Geophys. Res., 84*(64), 1797–1808, 1979*a*.

Grant, W. D., and O. S. Madsen, Bottom friction under waves in the presence of a weak current, *NOAA Tech. Rep., ERL-MESA*, 150 pp., Natl. Oceanic and Atmos. Admin., 1979*b*.

Hasselman, K., and J. I. Collins, Spectral dissipation of finite depth gravity waves due to turbulent bottom friction, *J. Mar. Res., 26*(1), 1–12, 1968.

Inman, D. L., Wave generated ripples in nearshore sands, *Tech. Memo. 100*, p. 41, U.S. Army Corps of Eng., Beach Erosion Board, 1957.

Jonsson, I. G., Wave boundary layers and friction factors, *Proc. Coastal Eng. Conf. 10th, 1*, 127–148, 1966.

Jonsson, I. G., and N. A. Carlsen, Experimental and theoretical investigations in an oscillatory turbulent boundary layer, *J. Hydraul. Res., 14*(1), 45–60, 1976.

Kajiura, K., On the bottom friction in an oscillatory current, *Bull. Earthquake Res. Inst. Univ. Tokyo, 42*, 147–174, 1964.

Kamphuis, J. W., Friction factor under oscillatory waves, *J. Waterways, Harbors Coastal Eng. Div., Am. Soc. Civ. Eng., 101*(WW2), 135–144, 1975.

Kobayashi, N., Turbulent flows over a wavy boundary and formation of bed forms in erodible channels, Ph.D. thesis, Dep. of Civil Eng., Mass. Inst. of Technol., Cambridge, Mass., 1979.

Lettau, H. H., Note on aerodynamic roughness-parameter estimation on the basis of roughness-element description, *J. Appl. Meterol., 8*, 828–832, 1969.

Luque, F. R., and V. R. Beek, Erosion and transport of bed load sediment, *J. Hydraul. Res., 14*(2), 127–144, 1976.

Madsen, O. S., and W. D. Grant, Sediment transport in the coastal environment, *Rep. 209,* 105 pp., Ralph M. Parson Lab., Dep. of Civil Eng., Mass. Inst. of Technol., Cambridge, Mass., 1976.

Madsen, O. S., and W. D. Grant, Quantitative description of sediment transport by waves, *Proc. Coastal Eng. Conf. 15th, II,* 1093–1112, 1977.

Millikan, C. B., A critical discussion of turbulent flow in channels and circular tubes, in *Proceedings of the Fifth International Congress on Applied Mechanics,* pp. 386–392, Wiley, New York, 1939.

Nikuradse, J., Strömungsgesetze in rauhen Rohren, *Forschungshefte 361,* VDI, 1933. (English translation, *NACA Tech. Memo. 1292,* Natl. Advis. Comm. for Aeronaut., Washington, D. C., 1950.)

Owen, P. R., Saltation of uniform grains in air, *J. Fluid Mech., 20*(2), 225, 1964.

Perry, A. E., W. H. Schofield, and P. N. Joubert, Rough wall turbulent boundary layers, *J. Fluid Mech., 37,* 383–413, 1969.

Putnam, J. A., and J. W. Johnson, The dissipation of wave energy by bottom friction, *Eos Trans. AGU, 30*(1), 67–74, 1949.

Shemdin, O., K. Hasselman, S. V. Hsiao, and K. Herterich, Nonlinear and linear bottom interaction effects in shallow water, in *Proceedings of NATO Symposium on Turbulent Fluxes Through the Sea Surface–Wave Dynamics and Prediction, Ile de Bendor, France,* pp. 12–16, Plenum, New York, 1977.

Smith, J. D., Modeling of sediment transport on continental shelves, in *The Sea,* vol. 6, Wiley-Interscience, New York, 1977.

Smith, J. D., and S. R. McLean, Spatially averaged flow over a wavy surface, *J. Geophys. Res., 82*(12), 1735–1746, 1977.

Swart, D. W., Predictive equations regarding coastal transports, *Proc. Coastal Eng. Conf. 15th, II,* 1113–1132, 1977.

Tennekes, H., and J. L. Lumley, *A First Course in Turbulence,* 300, pp., MIT Press, Cambridge, Mass., 1973.

Wooding, R. A., E. F. Bradley, and J. K. Marshall, Drag due to regular arrays of roughness elements of varying geometry, *Boundary Layer Meteorol., 5,* 285–308, 1973.

Yaglom, A. M., Similarity laws for constant-pressure and pressure-gradient turbulent wall flows, *Annu. Rev. Fluid Mech., 11,* 505–540, 1979.

(Received October 6, 1980;
revised September 8, 1981;
accepted September 15, 1981.)